

---

# PolUQBench: A Benchmark Study on Uncertainty Quantification of Polymer Property Prediction

---

Anonymous Author(s)

Affiliation

Address

email

## Abstract

1 Large Language Model(LLM)s have demonstrated remarkable capabilities to tackle  
2 multidomain challenges, a capability often lacking in conventional machine learn-  
3 ing methods. This makes them particularly promising for understanding the com-  
4 plex relationship between a material’s composition and its properties, which can  
5 significantly accelerate materials design, especially for polymers. Leveraging the  
6 hidden states of domain-specific pretrained LLMs for downstream tasks like prop-  
7 erty prediction has gained significant traction. This approach is now widely used for  
8 small molecules and proteins, along with recent efforts also extending to polymers.  
9 In addition to achieving superior predictive performance, Uncertainty Quantifica-  
10 tion (UQ) is another crucial aspect for enhancing the reliability of machine learning  
11 models used as property predictors. This is particularly important for high-stakes  
12 applications like the discovery of new functional polymers. We introduce **Polymer**  
13 **Property Predictor Uncertainty Quantification Benchmark**, a pioneering study that  
14 evaluates the effectiveness of embeddings extracted from a Polymer Language  
15 Model for representing polymer data and assesses the performance of several  
16 different UQ methods for reliable polymer property prediction.

## 17 1 Introduction

18 Language model embeddings are transforming how complex data is represented and used in science  
19 and engineering. These embedding techniques, which originated in Natural Language Processing  
20 to model linguistic relationships in a vector space, have demonstrated surprising utility across a  
21 wide range of disciplines. In bioinformatics, protein and genomic language models use sequence  
22 data to create embeddings that encode biological properties, enabling accurate predictions of protein  
23 function and structure [26, 37, 22]. Models like the ESM series [38, 23, 11, 6], have been shown  
24 to capture evolutionary and structural relationships directly from protein sequences, providing a  
25 powerful alternative to traditional feature engineering.

26 In materials science and chemistry, language models trained on chemical data (like SMILES) or text  
27 can produce embeddings that predict material properties, guide drug discovery, and accelerate the  
28 design of new compounds [44, 13]. These embeddings can encapsulate complex chemical knowledge,  
29 such as periodic table trends or structure-property relationships, in a vectorized format [44]. As a  
30 result, language model embeddings have unlocked new avenues for discovery and innovation by  
31 providing a unified and powerful representation for sequential and compositional data across a variety  
32 of domains.

33 The complex and diverse structures of polymers create unique challenges, despite their critical role in  
34 medical devices, energy storage, and aerospace engineering [9, 45, 25]. Accurate prediction of diverse  
35 polymer properties is essential for tailoring polymers to meet specific functional requirements [18].  
36 In contrast to time and resource-intensive traditional approaches for polymer property evaluation,

37 machine learning enables rapid, scalable, and cost-effective prediction of material properties, acceler-  
38 ating the development of advanced polymers for diverse applications [15, 52, 34, 30, 31, 49, 29]. By  
39 integrating data-driven insights with predictive accuracy, machine learning can streamline polymer  
40 discovery, optimize design, and transform polymer informatics [43].

41 Even after the tremendous success of ML polymer property predictors, relying solely on a single,  
42 deterministic prediction, also known as point estimate, is insufficient and potentially dangerous for  
43 high-stakes applications like polymer material design [40]. This critical limitation underscores the  
44 necessity for Uncertainty Quantification (UQ), a discipline dedicated to characterizing and quantifying  
45 the sources of uncertainty in predictive models [7]. Uncertainty Quantification is a critical enabler for  
46 trustworthy AI and scientific computing, as it provides the necessary confidence intervals that allow  
47 agents, human or automated, to make informed decisions, evaluate potential risks, and determine  
48 the credibility of a given prediction [53]. The two primary types of uncertainty that UQ methods  
49 aim to capture are *aleatoric* and *epistemic* uncertainty [42]. Aleatoric uncertainty is an irreducible  
50 property of the data generation process, arising from its inherent stochasticity. Conversely, epistemic  
51 uncertainty results from insufficient knowledge, often attributable to a model’s limited exposure to  
52 certain areas of the input space during training. This form of uncertainty is reducible in principle  
53 through the acquisition of more comprehensive training data [14].

54 Although machine learning has greatly advanced polymer property prediction, with a few works  
55 on benchmarking uncertainty quantification [41, 40], pioneering UQ benchmarking in the field still  
56 relies on traditional representations like Morgan fingerprints [32]. Consequently, there remains a  
57 critical gap in the literature regarding a systematic evaluation of modern polymer language model  
58 (PLM) embeddings for uncertainty quantification.

59 In this work, we introduce **Polymer property predictor Uncertainty Quantification Benchmark**  
60 (**PolUQBench**), an extensive benchmark for uncertainty quantification of ML polymer property  
61 predictors with Polymer Language Model embeddings as polymer representations. We utilize  
62 Polymer Prediction 2025 Dataset [24]. To the best of our knowledge, this is the most recent and  
63 extensive publicly available dataset for labeled polymer properties.

## 64 2 Problem Statement

65 The central problem addressed in this work is quantification of predictive uncertainty for machine  
66 learning polymer property predictors. Consider  $s_i$  be the SMILES representation of a polymer.  
67 Given a pretrained Polymer Language Model  $p_\phi$ , the hidden state embedding representation from the  
68 Polymer Language model is  $x_i = p_\phi(s_i)$ . We define a property predictor as a function  $f_\theta(x_i)$  that  
69 maps a polymer representation  $x_i$  to a predicted property  $\hat{y}_i$ . The goal of Uncertainty Quantification  
70 (UQ) is to complement this point prediction with an estimate of the probability distribution  $p(y_i|x_i, \mathcal{D})$   
71 over the possible true property values  $y_i$ , given the training data  $\mathcal{D}$ . This distribution can be  
72 summarized by its moments, most importantly the *Predictive Mean*,  $\mu(x_i)$  and *Predictive Variance*,  
73  $\sigma^2(x_i)$ :

$$\mu(x_i) = \mathbb{E}_{\theta \sim p(\theta|\mathcal{D})} f_\theta(x_i) \approx \hat{y}_i \quad (1)$$

$$\sigma^2(x_i) = \text{Var}_{\theta \sim p(\theta|\mathcal{D})} f_\theta(x_i) \quad (2)$$

75 The variance  $\sigma^2(x_i)$  captures the total predictive uncertainty.

## 76 3 PolUQBench

77 In this work, we focus on investigating UQ approaches in polymer property prediction tasks. This task  
78 can be cast as a regression problem, where the model is trained to predict some physical properties  
79 related to polymer. We first briefly describe the dataset we utilized in Section 3.1, the hidden state  
80 embedding extraction from Polymer Language models in Section 3.2, experimental setup in Section  
81 3.3 and experimental results in Section 3.4.

### 82 3.1 Dataset

83 We utilize Polymer Prediction 2025 Dataset [24], a large-scale open-source dataset. This dataset  
84 provides a polymer’s structure as a simple text string (SMILES) [46, 48, 47]. The set of labeled  
85 properties include: (i) *Density*, (ii) *Heat Thermal Conductivity* (Tc), (iii) *Glass Transition Temperature*  
86 (Tg), (iv) fundamental molecular size and packing efficiency *Radius of Gyration* (Rg) and (v)  
87 *Fractional Free Volume* (FFV). The ground truth for each property is averaged from multiple runs of  
88 molecular dynamics simulation.

## 89 3.2 Data Processing

90 We used two different Polymer Language Models (PLM) to extract embeddings that we utilize as  
91 input data for our property predictors: (i) *PolyNC* [35] and *PolyBERT* [19]. The PLM tokenizes  
92 the non-Hydrogen atoms and pass the tokens into the model. Considering length of the SMILES  
93 representation of the polymer is  $N$ , the size of the hidden state embedding of the PLM is  $N \times D$   
94 where  $D$  is the hidden state dimension. We averaged over the length of the hidden state dimension,  
95 resulting the polymer embedding dimension to be  $D$ . The value of  $D$  are 768 and 600 for *PolyNC*  
96 and *PolyBERT* accordingly.

## 97 3.3 Experimental Setup

98 **Architectural Setup:** We trained different models for each polymer property. For each property we  
99 conducted five-fold cross-validation experiments and report the evaluations on those five validation  
100 sets. We utilized the *LightningUQBox* [21] package to design and train all the different probabilistic  
101 models. For the backbone model, we employed a Fully Connected ResNet which is available in the  
102 *LightningUQBox* [21] package, with a hidden dimension of 256 and a depth of 8. All models were  
103 trained a total of 500 epochs, with a learning rate of 0.0001.

104 **Model:** Apart from deterministic model, we also evaluated the following set of probabilistic  
105 models in this benchmark: (i) MVE (Mean Variance Estimation) [33, 39], (ii) DEL (Deep Evidential  
106 Learning) [1, 28], (iii) QREG (Quantile Regression) [17], (iv) LA (Laplace Approximation) [36, 2],  
107 (v) MCD (Monte-Carlo Dropout) [8], (vi) MFVI (Mean Field Variational Inference) [16], (vii)  
108 BNNVI (Bayesian Neural Network with Variational Inference) [3], (viii) SWAG (Stochastic Weight  
109 Averaging Gaussian) [27], (ix) DKL (Deep Kernel Learning) [51], (x) VBLL (Variational Bayesian  
110 Last Layer) [10], (xi) VBLL SNGP (Variational Bayesian Last Layer (VBLL) with SNGP Regression),  
111 (xii) Deep Ensemble [20, 50], (xiii) Mask Ensemble [4], and (xiv) Zigzag [5].

112 **Evaluation Metrics:** To evaluate the models, we selected 4 metrics: (i) MAE (Mean Absolute  
113 Error), (ii) PCC (Pearson Correlation Coefficient), (iii) CRPS (Continuous Ranked Probability  
114 Score) [12] and (iv) CA (Calibration Area) [40]. The first 2 metrics evaluate the predictive perfor-  
115 mance of the model, and CRPS and CA are the UQ metrics.

## 116 3.4 Results

117 We report the evaluation metric values averaged over the five cross-validation splits for all polymer  
118 properties, and for both Polymer Language Models.

119 **Observations:** Table 1 shows the metric values for different models. For all properties, the  
120 probabilistic models obtained lower MAE than deterministic models, except for Tg with PolyNC  
121 embeddings. Unlike the case of MAE, the deterministic model obtained higher PCC values than  
122 probabilistic models for quite a lot of polymer properties. For most properties, the Mask Ensemble  
123 model obtained lower CRPS than other models. The VBLL SNGP model also obtained lowest CRPS  
124 value in some of the evaluation scenarios. For most properties, the MVE model obtained lowest CA  
125 than other models. Almost at all scenarios and for every metrics, models trained with PolyNC hidden  
126 state embeddings obtained better performances compared to models trained with PolyBERT hidden  
127 state embeddings.

128 **Discussion:** Experimental results indicate that a clear winner among the probabilistic models could  
129 not be identified, as no single model consistently outperformed the others across every metric. The  
130 probabilistic models consistently achieved a lower MAE than the deterministic baseline, signifying  
131 a general improvement in predictive accuracy. Additionally, a distinct performance advantage was  
132 observed for models trained with PolyNC hidden state embeddings over those trained with PolyBERT  
133 hidden state embeddings.

## 134 4 Conclusion

135 This work presented a pioneering benchmark study evaluating the efficacy of Polymer Language  
136 Model (PLM) embeddings for uncertainty quantification (UQ) in polymer property prediction.  
137 Diverging from prior UQ investigations that largely relied on conventional molecular fingerprints,  
138 such as Morgan fingerprints, our study uniquely leveraged the rich, contextual representations  
139 extracted from Protein Language Models. We evaluated a diverse set of probabilistic models across  
140 multiple polymer properties, providing a comprehensive characterization of predictive accuracy  
141 alongside robust uncertainty estimates.

Table 1: Evaluation Results.

MAE ( $\downarrow$ )										
Model	Density		Tc		Tg		Rg		FFV	
	PolyNC	PolyBERT								
BNN VI	0.0183	0.0216	0.0271	0.0292	0.1033	0.1132	0.0445	0.0456	0.0086	0.0100
Deep Ensemble	0.0194	0.0381	0.0278	0.0474	0.1035	0.1189	0.0443	0.0659	0.0222	0.0236
DEL	0.0280	0.0429	0.0354	0.0445	0.1274	0.1351	0.0585	0.0670	0.0129	0.0175
DKL	0.0294	0.0190	0.0306	0.0289	0.1229	0.1261	0.0494	0.0417	0.0079	0.0073
LA	0.0162	0.0194	0.0257	0.0274	<b>0.1000</b>	0.1050	0.0421	0.0400	0.0094	0.0112
Mask Ensemble	0.0165	<b>0.0183</b>	<b>0.0247</b>	<b>0.0260</b>	0.1126	0.1229	0.0412	<b>0.0395</b>	0.0089	0.0091
MC Dropout	0.0184	0.0194	0.0257	0.0277	0.1002	0.1070	0.0424	0.0403	0.0094	0.0112
MFVI	0.0178	0.0213	0.0275	0.0290	0.1245	0.1433	0.0445	0.0453	0.0196	0.0210
MVE	0.0195	0.1206	0.0271	0.0631	0.1041	0.1077	0.0418	0.0899	0.0162	0.0520
QREG	<b>0.0151</b>	0.0196	0.0256	0.0278	0.1018	0.1104	0.0411	0.0411	0.0079	0.0120
SWAG	0.0168	0.0190	0.0254	0.0271	0.1020	0.1086	0.0415	0.0421	0.0090	0.0104
VBLL	0.0445	0.0655	0.0375	0.0636	0.1151	0.1314	0.0583	0.0750	0.0088	0.0097
VBLL SNGP	0.1351	0.0899	0.0716	0.1134	0.1226	<b>0.1048</b>	0.1377	0.1807	<b>0.0060</b>	<b>0.0069</b>
ZigZag	0.0164	0.0186	0.0255	0.0271	0.1017	0.1076	<b>0.0410</b>	0.0416	0.0085	0.0108
Deterministic	0.0162	0.0194	0.0257	0.0274	<b>0.1000</b>	0.1050	0.0421	0.0400	0.0094	0.0112
PCC ( $\uparrow$ )										
Model	Density		Tc		Tg		Rg		FFV	
	PolyNC	PolyBERT								
BNN VI	0.9102	0.8970	0.9019	0.8925	0.8013	0.7481	0.8448	0.8419	0.8918	0.8451
Deep Ensemble	0.9004	0.7085	0.9011	0.8037	0.8026	0.7153	0.8438	0.7419	0.7446	0.4683
DEL	0.9010	0.8474	0.8826	0.8664	0.7066	0.6715	0.8307	0.8208	0.7938	0.6763
DKL	0.8866	<b>0.9174</b>	0.8769	0.8884	0.7187	0.6906	0.8406	0.8446	0.9088	0.9229
LA	<b>0.9265</b>	0.9156	0.9109	<b>0.9017</b>	0.8069	0.7814	0.8606	<b>0.8694</b>	0.8697	0.8093
Mask Ensemble	0.9072	0.9006	0.9075	0.8982	0.7610	0.6904	0.8512	0.8624	0.8316	0.8551
MC Dropout	0.9223	0.9155	0.9104	0.8989	<b>0.8078</b>	0.7757	0.8600	0.8674	0.8690	0.8077
MFVI	0.9180	0.8955	0.9002	0.8890	0.7169	0.6342	0.8444	0.8370	0.6124	0.5734
MVE	0.9060	0.2897	0.9089	0.6502	0.7994	0.7684	0.8628	0.6049	0.7285	0.3875
QREG	0.9254	0.9068	0.9046	0.8957	0.8004	0.7599	0.8627	0.8637	0.8838	0.7893
SWAG	0.9250	0.9145	<b>0.9109</b>	0.9004	0.8073	0.7794	0.8604	0.8634	0.8722	0.8253
VBLL	0.7881	0.4882	0.8913	0.6933	0.7722	0.6866	0.8050	0.6161	0.9119	0.8708
VBLL SNGP	0.5392	0.7400	0.6827	0.5918	0.6397	0.7763	0.5622	0.5518	<b>0.9409</b>	<b>0.9282</b>
ZigZag	0.9205	0.9140	0.9095	0.9017	0.8073	<b>0.7816</b>	<b>0.8643</b>	0.8653	0.8980	0.8506
Deterministic	<b>0.9265</b>	0.9156	0.9109	<b>0.9017</b>	0.8069	0.7814	0.8606	<b>0.8694</b>	0.8697	0.8093
CRPS ( $\downarrow$ )										
Model	Density		Tc		Tg		Rg		FFV	
	PolyNC	PolyBERT								
BNN VI	0.0169	0.0192	0.0256	0.0272	0.1011	0.1059	0.0429	0.0425	0.0077	0.0084
Deep Ensemble	0.0162	0.0299	0.0221	0.0324	0.0875	0.0905	0.0365	0.0466	0.0129	0.0201
DEL	0.1286	0.1443	0.1297	0.1403	0.1645	0.1775	0.1415	0.1539	0.0993	0.1187
DKL	0.0213	0.0149	0.0230	0.0219	0.0920	0.0999	0.0368	0.0326	0.0068	0.0064
LA	0.0158	0.0191	0.0256	0.0271	0.0994	0.1017	0.0420	0.0396	0.0094	0.0111
Mask Ensemble	<b>0.0119</b>	<b>0.0134</b>	<b>0.0181</b>	<b>0.0193</b>	0.0834	0.0930	<b>0.0301</b>	<b>0.0287</b>	0.0064	0.0066
MC Dropout	0.0140	0.0143	0.0194	0.0206	0.0770	0.0784	0.0315	0.0304	0.0069	0.0083
MFVI	0.0206	0.0234	0.0251	0.0274	0.0972	0.1116	0.0397	0.0400	0.2406	0.2451
MVE	0.0164	0.1276	0.0207	0.0982	0.0736	0.0766	0.0312	0.0983	0.1397	0.2399
QREG	0.0117	0.0152	0.0189	0.0213	<b>0.0738</b>	0.0807	0.0304	0.0306	0.0061	0.0093
SWAG	0.0152	0.0178	0.0247	0.0261	0.0996	0.1042	0.0406	0.0399	0.0087	0.0098
VBLL	0.1212	0.1353	0.0688	0.1311	0.1917	0.1590	0.1099	0.1419	0.0081	0.0081
VBLL SNGP	0.0982	0.0578	0.0478	0.0734	0.0913	<b>0.0765</b>	0.0981	0.1155	<b>0.0046</b>	<b>0.0052</b>
ZigZag	0.0147	0.0172	0.0228	0.0253	0.0919	0.0951	0.0364	0.0397	0.0076	0.0096
CA ( $\downarrow$ )										
Model	Density		Tc		Tg		Rg		FFV	
	PolyNC	PolyBERT								
BNN VI	0.0635	0.1315	0.1510	<b>0.0213</b>	0.2896	0.3011	0.1461	0.0735	0.0858	0.0513
Deep Ensemble	0.1663	0.2641	<b>0.0230</b>	0.2215	0.1611	0.1034	0.0528	0.1329	0.4517	0.4577
DEL	0.4170	0.3884	0.3971	0.3798	0.2019	0.2092	0.3457	0.3362	0.4487	0.4428
DKL	0.1860	0.0856	0.1818	0.2191	0.2899	0.3256	0.2223	0.2119	<b>0.0394</b>	0.0462
LA	0.4687	0.4705	0.4717	0.4728	0.4693	0.4557	0.4747	0.4691	0.4750	0.4744
Mask Ensemble	0.1932	0.1437	0.2151	0.1911	0.2422	0.2953	0.2080	0.2146	0.1297	0.1234
MC Dropout	0.1035	0.1650	0.2075	0.1930	0.3005	0.2130	0.2708	0.2165	0.1970	0.1637
MFVI	0.1823	0.1595	0.0668	0.0911	<b>0.0451</b>	<b>0.0627</b>	<b>0.0521</b>	<b>0.0517</b>	0.4652	0.4637
MVE	<b>0.0398</b>	0.1205	0.0827	0.1760	0.1906	0.1919	0.1044	0.1207	0.2964	0.4181
QREG	0.0977	<b>0.0790</b>	0.1710	0.1130	0.1620	0.1596	0.1554	0.1350	0.0912	0.0698
SWAG	0.4085	0.4405	0.4607	0.4610	0.4642	0.4594	0.4618	0.4498	0.4577	0.4443
VBLL	0.3565	0.3174	0.2869	0.3164	0.2722	0.1834	0.2945	0.3002	0.0698	<b>0.0228</b>
VBLL SNGP	0.0741	0.1447	0.1732	0.2197	0.1241	0.1573	0.1188	0.2109	0.1095	0.1502
ZigZag	0.3765	0.4226	0.4112	0.4329	0.4307	0.4139	0.3985	0.4547	0.4185	0.4116

## References

- [1] A. Amini, W. Schwarting, A. Soleimany, and D. Rus. Deep evidential regression. *Advances in neural information processing systems*, 33:14927–14937, 2020.
- [2] E. Daxberger, E. Nalisnick, J. U. Allingham, J. Antorán, and J. M. Hernández-Lobato. Bayesian deep learning via subnetwork inference. In *International Conference on Machine Learning*, pages 2510–2521. PMLR, 2021.
- [3] S. Depeweg, J.-M. Hernandez-Lobato, F. Doshi-Velez, and S. Udluft. Decomposition of uncertainty in bayesian deep learning for efficient and risk-sensitive learning. In *International conference on machine learning*, pages 1184–1193. PMLR, 2018.
- [4] N. Durasov, T. Bagautdinov, P. Baque, and P. Fua. Masksembles for uncertainty estimation. In *Proceedings of the IEEE/CVF Conference on Computer Vision and Pattern Recognition*, pages 13539–13548, 2021.
- [5] N. Durasov, N. Dorndorf, H. Le, and P. Fua. Zigzag: Universal sampling-free uncertainty estimation through two-step inference. *Transactions on Machine Learning Research*, 2024. ISSN 2835-8856. URL <https://openreview.net/forum?id=QSvb6jBXML>.
- [6] ESM Team. Esm cambrian: Revealing the mysteries of proteins with unsupervised learning, 2024. URL <https://evolutionaryscale.ai/blog/esm-cambrian>.
- [7] Y. Gal. *Uncertainty in Deep Learning*. PhD thesis, University of Cambridge, 2016.
- [8] Y. Gal and Z. Ghahramani. Dropout as a bayesian approximation: Representing model uncertainty in deep learning. In *international conference on machine learning*, pages 1050–1059. PMLR, 2016.
- [9] P. L. Golas and K. Matyjaszewski. Marrying click chemistry with polymerization: expanding the scope of polymeric materials. *Chem. Soc. Rev.*, 39(4):1338–1354, 2010. ISSN 1460-4744. doi: 10.1039/b901978m. URL <http://dx.doi.org/10.1039/B901978M>.
- [10] J. Harrison, J. Willes, and J. Snoek. Variational bayesian last layers. In *International Conference on Learning Representations (ICLR)*, 2024.
- [11] T. Hayes, R. Rao, H. Akin, N. J. Sofroniew, D. Oktay, Z. Lin, R. Verkuil, V. Q. Tran, J. Deaton, M. Wiggert, R. Badkundri, I. Shafkat, J. Gong, A. Derry, R. S. Molina, N. Thomas, Y. A. Khan, C. Mishra, C. Kim, L. J. Bartie, M. Nemeth, P. D. Hsu, T. Sercu, S. Candido, and A. Rives. Simulating 500 million years of evolution with a language model. *Science*, 387(6736): 850–858, 2025. doi: 10.1126/science.ads0018. URL <https://www.science.org/doi/abs/10.1126/science.ads0018>.
- [12] H. Hersbach. Decomposition of the continuous ranked probability score for ensemble prediction systems. *Weather and Forecasting*, 15(5):559–570, Oct. 2000. ISSN 1520-0434. doi: 10.1175/1520-0434(2000)015<0559:dotcrp>2.0.co;2. URL [http://dx.doi.org/10.1175/1520-0434\(2000\)015<0559:DOTCRP>2.0.CO;2](http://dx.doi.org/10.1175/1520-0434(2000)015<0559:DOTCRP>2.0.CO;2).
- [13] C. Jin, S. Guo, S. Zhou, and J. Guan. Effective and explainable molecular property prediction by chain-of-thought enabled large language models and multi-modal molecular information fusion. *Journal of Chemical Information and Modeling*, 65(11):5438–5455, 2025. doi: 10.1021/acs.jcim.5c00577. URL <https://doi.org/10.1021/acs.jcim.5c00577>. PMID: 40392109.
- [14] A. Kendall and Y. Gal. What uncertainties do we need in bayesian deep learning for computer vision? *Advances in neural information processing systems*, 30, 2017.
- [15] C. Kim, A. Chandrasekaran, T. D. Huan, D. Das, and R. Ramprasad. Polymer genome: A data-powered polymer informatics platform for property predictions. *The Journal of Physical Chemistry C*, 122(31):17575–17585, July 2018. ISSN 1932-7455. doi: 10.1021/acs.jpcc.8b02913. URL <http://dx.doi.org/10.1021/acs.jpcc.8b02913>.
- [16] D. P. Kingma and M. Welling. Auto-encoding variational bayes. *arXiv preprint arXiv:1312.6114*, 2013.

- 190 [17] R. Koenker and G. Bassett. Regression quantiles. *Econometrica*, 46(1):33, Jan. 1978. ISSN  
191 0012-9682. doi: 10.2307/1913643. URL <http://dx.doi.org/10.2307/1913643>.
- 192 [18] D. V. Krevelen. *Properties of Polymers; Their Correlation with Chemical Structure; Their*  
193 *Numerical Estimation and Prediction from Additive Group Contributions*. Elsevier, 1997. ISBN  
194 9780444828774. doi: 10.1016/c2009-0-05459-2.
- 195 [19] C. Kuenneth and R. Ramprasad. polybert: a chemical language model to enable fully  
196 machine-driven ultrafast polymer informatics. *Nature Communications*, 14(1), July 2023.  
197 ISSN 2041-1723. doi: 10.1038/s41467-023-39868-6. URL <http://dx.doi.org/10.1038/s41467-023-39868-6>.
- 199 [20] B. Lakshminarayanan, A. Pritzel, and C. Blundell. Simple and scalable predictive uncertainty  
200 estimation using deep ensembles. *Advances in neural information processing systems*, 30, 2017.
- 201 [21] N. Lehmann, N. M. Gottschling, J. Gawlikowski, A. J. Stewart, S. Depeweg, and E. Nalisnick.  
202 Lightning uq box: Uncertainty quantification for neural networks. *Journal of Machine Learning*  
203 *Research*, 26(54):1–7, 2025. URL <http://jmlr.org/papers/v26/24-2110.html>.
- 204 [22] S. Li, Y. Tan, S. Ke, L. Hong, and B. Zhou. Immunogenicity prediction with dual attention  
205 enables vaccine target selection. In *The Thirteenth International Conference on Learning*  
206 *Representations*, 2025. URL <https://openreview.net/forum?id=hWmwL9gizZ>.
- 207 [23] Z. Lin, H. Akin, R. Rao, B. Hie, Z. Zhu, W. Lu, N. Smetanin, R. Verkuil, O. Kabeli, Y. Shmueli,  
208 A. dos Santos Costa, M. Fazel-Zarandi, T. Sercu, S. Candido, and A. Rives. Evolutionary-scale  
209 prediction of atomic-level protein structure with a language model. *Science*, 379(6637):1123–  
210 1130, 2023. doi: 10.1126/science.ade2574. URL <https://www.science.org/doi/abs/10.1126/science.ade2574>.
- 212 [24] G. Liu, J. Xu, E. Inae, Y. Zhu, Y. Li, T. Luo, M. Jiang, Y. Yan, W. Reade, S. Dane, A. Howard, and  
213 M. Cruz. Neurips - open polymer prediction 2025. [https://kaggle.com/competitions/](https://kaggle.com/competitions/neurips-open-polymer-prediction-2025)  
214 [neurips-open-polymer-prediction-2025](https://kaggle.com/competitions/neurips-open-polymer-prediction-2025), 2025. Kaggle.
- 215 [25] Y. Liu, H. Du, L. Liu, and J. Leng. Shape memory polymers and their composites in aerospace  
216 applications: a review. *Smart Materials and Structures*, 23(2):023001, Jan. 2014. ISSN  
217 1361-665X. doi: 10.1088/0964-1726/23/2/023001. URL [http://dx.doi.org/10.1088/](http://dx.doi.org/10.1088/0964-1726/23/2/023001)  
218 [0964-1726/23/2/023001](http://dx.doi.org/10.1088/0964-1726/23/2/023001).
- 219 [26] S. Madan, M. Lentzen, J. Brandt, D. Rueckert, M. Hofmann-Apitius, and H. Fröhlich. Trans-  
220 former models in biomedicine. *BMC Medical Informatics and Decision Making*, 24(1), July  
221 2024. ISSN 1472-6947. doi: 10.1186/s12911-024-02600-5. URL [http://dx.doi.org/10.](http://dx.doi.org/10.1186/s12911-024-02600-5)  
222 [1186/s12911-024-02600-5](http://dx.doi.org/10.1186/s12911-024-02600-5).
- 223 [27] W. J. Maddox, P. Izmailov, T. Garipov, D. P. Vetrov, and A. G. Wilson. A simple baseline for  
224 bayesian uncertainty in deep learning. *Advances in neural information processing systems*, 32,  
225 2019.
- 226 [28] N. Meinert, J. Gawlikowski, and A. Lavin. The unreasonable effectiveness of deep evidential  
227 regression. *Proceedings of the AAAI Conference on Artificial Intelligence*, 37(8):9134–9142,  
228 Jun. 2023. doi: 10.1609/aaai.v37i8.26096. URL [https://ojs.aaai.org/index.php/](https://ojs.aaai.org/index.php/AAAI/article/view/26096)  
229 [AAAI/article/view/26096](https://ojs.aaai.org/index.php/AAAI/article/view/26096).
- 230 [29] L. A. Miccio and G. A. Schwartz. From chemical structure to quantitative polymer properties  
231 prediction through convolutional neural networks. *Polymer*, 193:122341, 2020. ISSN 0032-3861.  
232 doi: <https://doi.org/10.1016/j.polymer.2020.122341>. URL [https://www.sciencedirect.](https://www.sciencedirect.com/science/article/pii/S0032386120301786)  
233 [com/science/article/pii/S0032386120301786](https://www.sciencedirect.com/science/article/pii/S0032386120301786).
- 234 [30] L. A. Miccio and G. A. Schwartz. Localizing and quantifying the intra-monomer contributions  
235 to the glass transition temperature using artificial neural networks. *Polymer*, 203:122786,  
236 2020. ISSN 0032-3861. doi: <https://doi.org/10.1016/j.polymer.2020.122786>. URL [https://www.sciencedirect.](https://www.sciencedirect.com/science/article/pii/S0032386120306145)  
237 [com/science/article/pii/S0032386120306145](https://www.sciencedirect.com/science/article/pii/S0032386120306145).

- 238 [31] L. A. Miccio and G. A. Schwartz. Mapping chemical structure–glass transition temperature  
239 relationship through artificial intelligence. *Macromolecules*, 54(4):1811–1817, 2021. doi: 10.  
240 1021/acs.macromol.0c02594. URL <https://doi.org/10.1021/acs.macromol.0c02594>.
- 241 [32] H. L. Morgan. The generation of a unique machine description for chemical structures—a  
242 technique developed at chemical abstracts service. *Journal of Chemical Documentation*, 5(2):  
243 107–113, May 1965. ISSN 1541-5732. doi: 10.1021/c160017a018. URL <http://dx.doi.org/10.1021/c160017a018>.
- 245 [33] D. Nix and A. Weigend. Estimating the mean and variance of the target probability distribu-  
246 tion. In *Proceedings of 1994 IEEE International Conference on Neural Networks (ICNN'94)*,  
247 volume 1, pages 55–60 vol.1, 1994. doi: 10.1109/ICNN.1994.374138.
- 248 [34] G. Pilania, C. N. Iverson, T. Lookman, and B. L. Marrone. Machine-learning-based predictive  
249 modeling of glass transition temperatures: A case of polyhydroxyalkanoate homopolymers and  
250 copolymers. *Journal of Chemical Information and Modeling*, 59(12):5013–5025, 2019. doi:  
251 10.1021/acs.jcim.9b00807. URL <https://doi.org/10.1021/acs.jcim.9b00807>. PMID:  
252 31697891.
- 253 [35] H. Qiu, L. Liu, X. Qiu, X. Dai, X. Ji, and Z.-Y. Sun. Polync: a natural and chemical language  
254 model for the prediction of unified polymer properties. *Chemical Science*, 15(2):534–544,  
255 2024. ISSN 2041-6539. doi: 10.1039/d3sc05079c. URL [http://dx.doi.org/10.1039/](http://dx.doi.org/10.1039/D3SC05079C)  
256 [D3SC05079C](http://dx.doi.org/10.1039/D3SC05079C).
- 257 [36] H. Ritter, A. Botev, and D. Barber. A scalable laplace approximation for neural networks. In  
258 *International Conference on Learning Representations*, 2018. URL <https://openreview.net/forum?id=Skdvd2xAZ>.
- 260 [37] A. Rives, J. Meier, T. Sercu, S. Goyal, Z. Lin, J. Liu, D. Guo, M. Ott, C. L. Zitnick, J. Ma,  
261 and R. Fergus. Biological structure and function emerge from scaling unsupervised learning  
262 to 250 million protein sequences. *Proceedings of the National Academy of Sciences*, 118(15):  
263 e2016239118, 2021. doi: 10.1073/pnas.2016239118. URL [https://www.pnas.org/doi/](https://www.pnas.org/doi/abs/10.1073/pnas.2016239118)  
264 [abs/10.1073/pnas.2016239118](https://www.pnas.org/doi/abs/10.1073/pnas.2016239118).
- 265 [38] A. Rives, J. Meier, T. Sercu, S. Goyal, Z. Lin, J. Liu, D. Guo, M. Ott, C. L. Zitnick, J. Ma,  
266 and R. Fergus. Biological structure and function emerge from scaling unsupervised learning  
267 to 250 million protein sequences. *Proceedings of the National Academy of Sciences*, 118(15):  
268 e2016239118, 2021. doi: 10.1073/pnas.2016239118. URL [https://www.pnas.org/doi/](https://www.pnas.org/doi/abs/10.1073/pnas.2016239118)  
269 [abs/10.1073/pnas.2016239118](https://www.pnas.org/doi/abs/10.1073/pnas.2016239118).
- 270 [39] L. Sluijterman, E. Cator, and T. Heskes. Optimal training of mean variance estimation neural  
271 networks. *Neurocomputing*, 597:127929, 2024. ISSN 0925-2312. doi: [https://doi.org/10.1016/j.](https://doi.org/10.1016/j.neucom.2024.127929)  
272 [neucom.2024.127929](https://doi.org/10.1016/j.neucom.2024.127929). URL [https://www.sciencedirect.com/science/article/pii/](https://www.sciencedirect.com/science/article/pii/S0925231224007008)  
273 [S0925231224007008](https://www.sciencedirect.com/science/article/pii/S0925231224007008).
- 274 [40] H. Tang, T. Yue, and Y. Li. Assessing uncertainty in machine learning for polymer property  
275 prediction: A benchmark study. *Journal of Chemical Information and Modeling*, 65(13):6585–  
276 6598, 2025. doi: 10.1021/acs.jcim.5c00550. URL [https://doi.org/10.1021/acs.jcim.](https://doi.org/10.1021/acs.jcim.5c00550)  
277 [5c00550](https://doi.org/10.1021/acs.jcim.5c00550). PMID: 40560148.
- 278 [41] L. Tao, V. Varshney, and Y. Li. Benchmarking machine learning models for polymer informatics:  
279 An example of glass transition temperature. *Journal of Chemical Information and Modeling*,  
280 61(11):5395–5413, Oct. 2021. ISSN 1549-960X. doi: 10.1021/acs.jcim.1c01031. URL  
281 <http://dx.doi.org/10.1021/acs.jcim.1c01031>.
- 282 [42] F. Tavazza, B. DeCost, and K. Choudhary. Uncertainty prediction for machine learning models  
283 of material properties. *ACS omega*, 6(48):32431–32440, 2021.
- 284 [43] H. Tran, R. Gurnani, C. Kim, G. Pilania, H.-K. Kwon, R. P. Lively, and R. Ramprasad. Design  
285 of functional and sustainable polymers assisted by artificial intelligence. *Nature Reviews*  
286 *Materials*, 9(12):866–886, Aug. 2024. ISSN 2058-8437. doi: 10.1038/s41578-024-00708-8.  
287 URL <http://dx.doi.org/10.1038/s41578-024-00708-8>.

- 288 [44] V. Tshitoyan, J. Dagdelen, L. Weston, A. Dunn, Z. Rong, O. Kononova, K. A. Persson,  
289 G. Ceder, and A. Jain. Unsupervised word embeddings capture latent knowledge from  
290 materials science literature. *Nature*, 571(7763):95–98, July 2019. ISSN 1476-4687. doi:  
291 10.1038/s41586-019-1335-8. URL <http://dx.doi.org/10.1038/s41586-019-1335-8>.
- 292 [45] B. D. Ulery, L. S. Nair, and C. T. Laurencin. Biomedical applications of biodegradable polymers.  
293 *Journal of Polymer Science Part B: Polymer Physics*, 49(12):832–864, May 2011. ISSN 1099-  
294 0488. doi: 10.1002/polb.22259. URL <http://dx.doi.org/10.1002/polb.22259>.
- 295 [46] D. Weininger. Smiles, a chemical language and information system. 1. introduction to  
296 methodology and encoding rules. *Journal of Chemical Information and Computer Sci-*  
297 *ences*, 28(1):31–36, Feb. 1988. ISSN 1520-5142. doi: 10.1021/ci00057a005. URL  
298 <http://dx.doi.org/10.1021/ci00057a005>.
- 299 [47] D. Weininger. Smiles. 3. depict. graphical depiction of chemical structures. *Journal of Chemical*  
300 *Information and Computer Sciences*, 30(3):237–243, Aug. 1990. ISSN 1520-5142. doi:  
301 10.1021/ci00067a005. URL <http://dx.doi.org/10.1021/ci00067a005>.
- 302 [48] D. Weininger, A. Weininger, and J. L. Weininger. Smiles. 2. algorithm for generation of unique  
303 smiles notation. *Journal of Chemical Information and Computer Sciences*, 29(2):97–101, May  
304 1989. ISSN 1520-5142. doi: 10.1021/ci00062a008. URL <http://dx.doi.org/10.1021/ci00062a008>.
- 306 [49] B. K. Wheatle, E. F. Fuentes, N. A. Lynd, and V. Ganesan. Design of polymer blend electrolytes  
307 through a machine learning approach. *Macromolecules*, 53(21):9449–9459, 2020. doi: 10.1021/  
308 acs.macromol.0c01547. URL <https://doi.org/10.1021/acs.macromol.0c01547>.
- 309 [50] A. G. Wilson and P. Izmailov. Bayesian deep learning and a probabilistic perspective of  
310 generalization. *Advances in neural information processing systems*, 33:4697–4708, 2020.
- 311 [51] A. G. Wilson, Z. Hu, R. Salakhutdinov, and E. P. Xing. Deep kernel learning. In *Artificial*  
312 *intelligence and statistics*, pages 370–378. PMLR, 2016.
- 313 [52] S. Wu, Y. Kondo, M.-a. Kakimoto, B. Yang, H. Yamada, I. Kuwajima, G. Lambard, K. Hongo,  
314 Y. Xu, J. Shiomi, C. Schick, J. Morikawa, and R. Yoshida. Machine-learning-assisted discovery  
315 of polymers with high thermal conductivity using a molecular design algorithm. *npj Computa-*  
316 *tional Materials*, 5(1), June 2019. ISSN 2057-3960. doi: 10.1038/s41524-019-0203-2. URL  
317 <http://dx.doi.org/10.1038/s41524-019-0203-2>.
- 318 [53] N. Zhan and J. R. Kitchin. Uncertainty quantification in machine learning and nonlinear  
319 least squares regression models. *AIChE Journal*, 68(6), Nov. 2021. ISSN 1547-5905. doi:  
320 10.1002/aic.17516. URL <http://dx.doi.org/10.1002/aic.17516>.

321 **A Evaluation Metrics**

322 **Mean Absolute Error (MAE):** Considering the trained property predictor model  $f_\theta$ , the polymer  
 323 representation  $x$ , and the ground truth property value  $y$ , the MAE metric is evaluated as:

$$\text{MAE}(\mathbf{x}, \mathbf{y}) = \frac{1}{n} \sum_{i=1}^n |f_\theta(x_i) - y_i| \tag{3}$$

324 **Pearson Correlation Coefficient (PCC):** Considering the trained property predictor model  $f_\theta$ , the  
 325 test set polymer representation  $\mathbf{x}$ , and the ground truth property value of test set  $\mathbf{y}$ , and the predicted  
 326 property values of test set  $\hat{\mathbf{y}}$ , the PCC metric is evaluated as:

$$\text{PCC}(\hat{\mathbf{y}}, \mathbf{y}) = \frac{\text{Cov}(\hat{\mathbf{y}}, \mathbf{y})}{\text{Var}(\mathbf{y})\text{Var}(\hat{\mathbf{y}})} \tag{4}$$

327 **Continuous Ranked Probability Score (CRPS):** Considering the trained property predictor model  
 328  $f_\theta$ , the polymer representation  $x$ , and the ground truth property value  $y$ , the CRPS metric is evaluated  
 329 as:

$$\text{CRPS}(f_\theta(x_i), y_i) = \int_{-\infty}^{\infty} [\Phi(f_\theta(x_i)) - 1_{f_\theta(x_i) \geq y_i}]^2 df_\theta(x_i), \tag{5}$$

330 Here  $\Phi(f_\theta(x_i))$  is the cumulative distribution function of the predictive distribution  $f_\theta(x_i)$ . To  
 331 evaluate CRPS over the full test set  $(\mathbf{x}, \mathbf{y})$ , we take the average over the CRPS for each sample in the  
 332 test set:

$$\text{CRPS}(f_\theta, \mathbf{x}, \mathbf{y}) = \frac{1}{n} \sum_i \text{CRPS}(f_\theta(x_i), y_i) \tag{6}$$

333 **Calibration Area (CA):** We follow the definition of CA metric defined in Tang et al. [40]. The  
 334 process for evaluating this metric involves constructing confidence intervals based on uncertainty  
 335 estimates and then determining the proportion of true values that lie within these intervals. Plotting  
 336 the observed confidence against the expected confidence yields the calibration curve. A well-  
 337 calibrated model’s curve will align with the diagonal, while deviations reveal overconfidence (below  
 338 the diagonal) or under-confidence (above the diagonal). The CA metric is the area between the  
 339 calibration curve and the diagonal.

340 **B Additional Results**

341 To show the variability of our results, we’ve created bar plots for all models and polymer properties,  
 342 illustrating the range of metric values over the five cross-validation splits. The value on each bar  
 343 represents the median value among the metrics for the cross-validation splits.

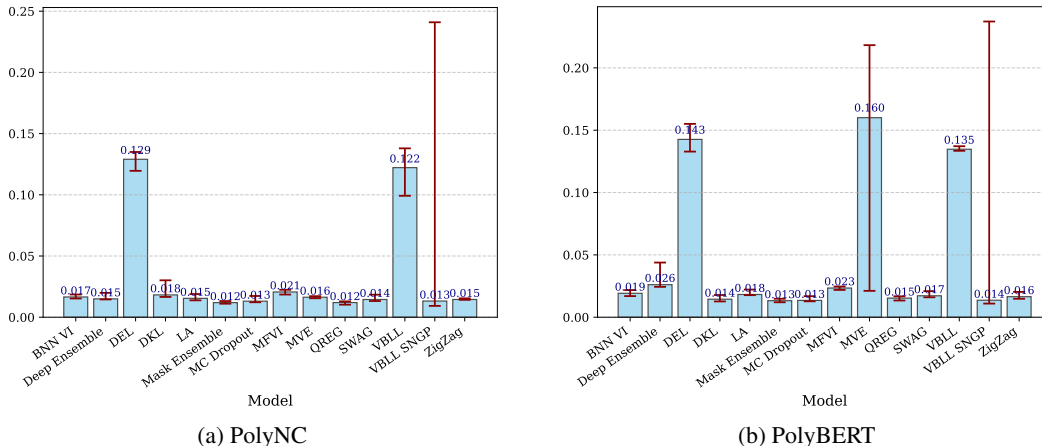
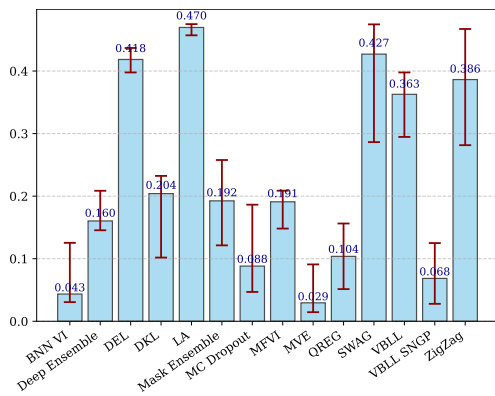
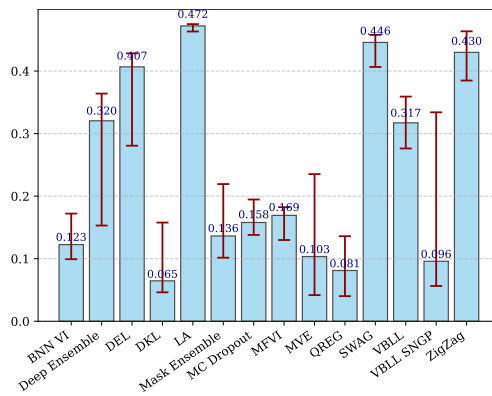


Figure 1: CRPS values for Density property of polymers.

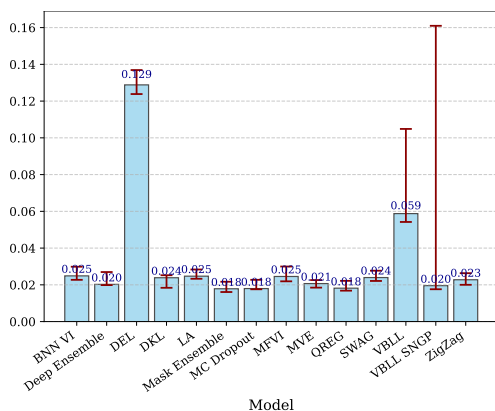


(a) PolyNC

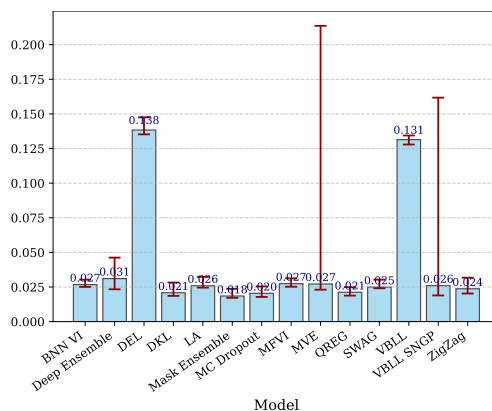


(b) PolyBERT

Figure 2: CA values for Density property of polymers.

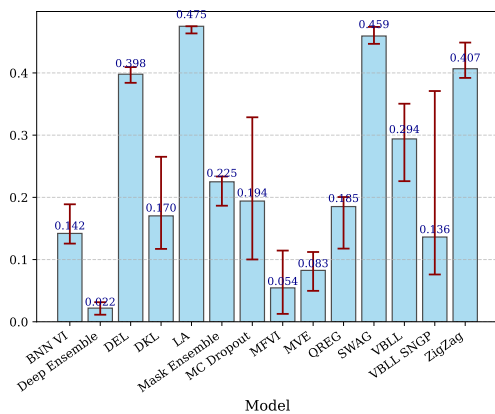


(a) PolyNC

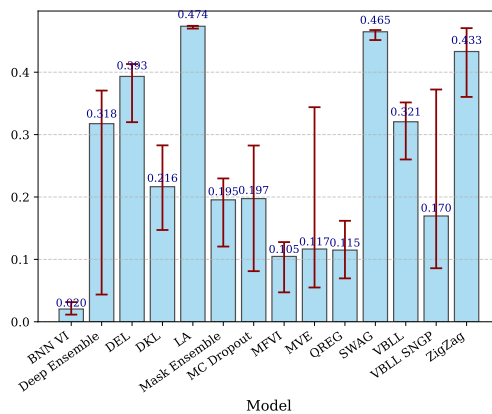


(b) PolyBERT

Figure 3: CRPS values for Tc property of polymers.

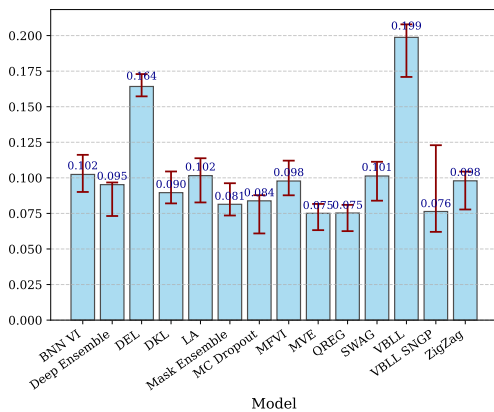


(a) PolyNC

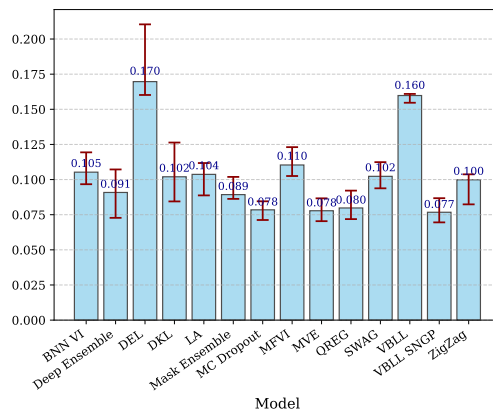


(b) PolyBERT

Figure 4: CA values for Tc property of polymers.

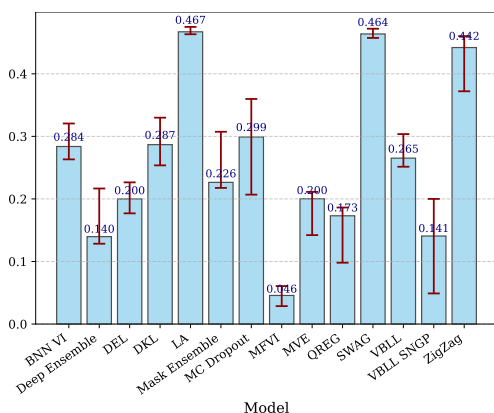


(a) PolyNC

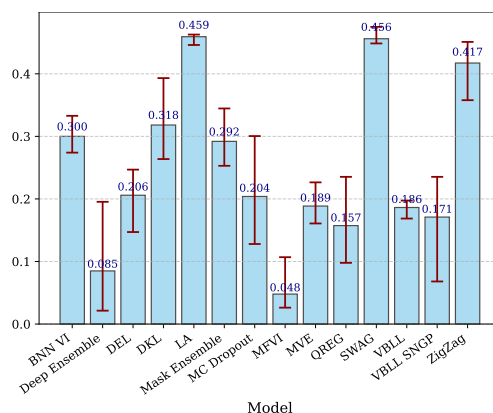


(b) PolyBERT

Figure 5: CRPS values for Tg property of polymers.

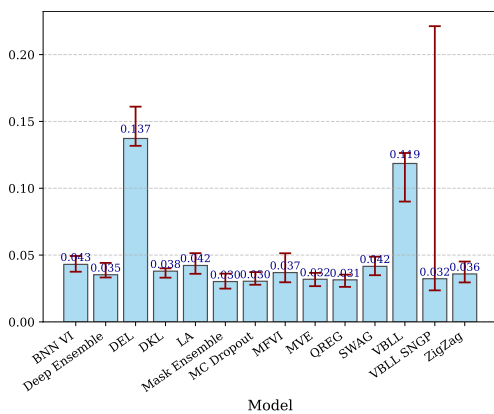


(a) PolyNC

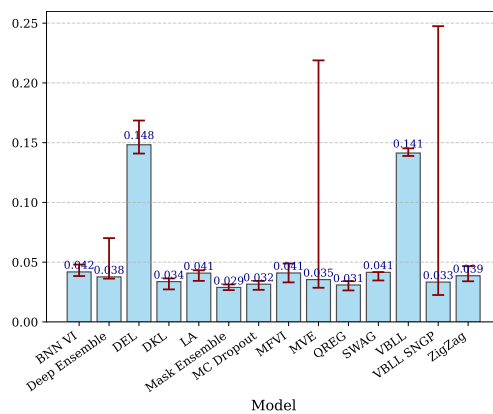


(b) PolyBERT

Figure 6: CA values for Tg property of polymers.

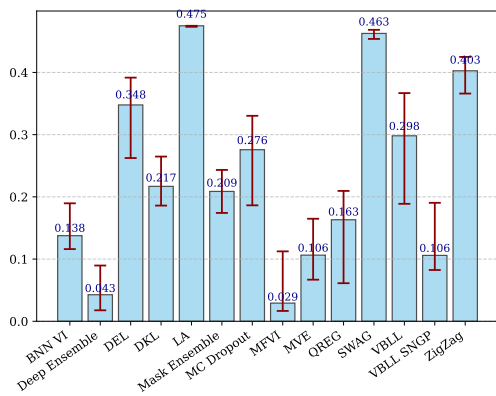


(a) PolyNC

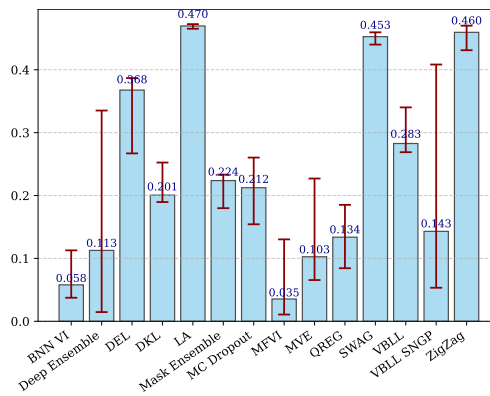


(b) PolyBERT

Figure 7: CRPS values for Rg property of polymers.

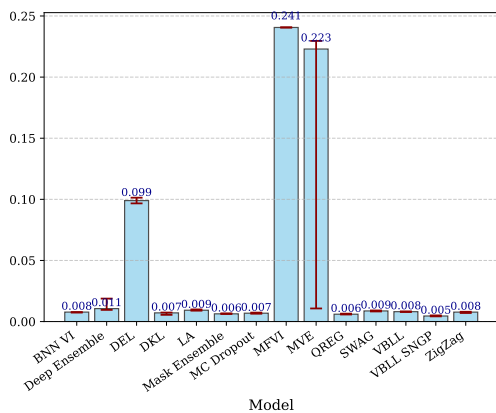


(a) PolyNC

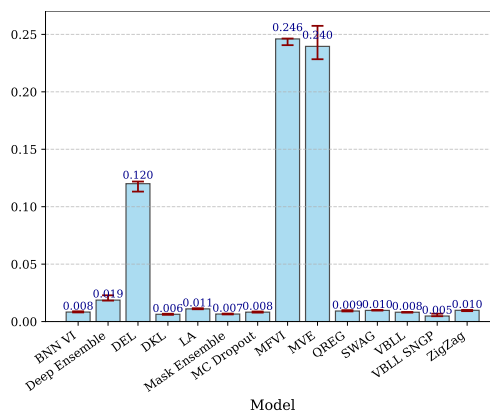


(b) PolyBERT

Figure 8: CA values for Rg property of polymers.

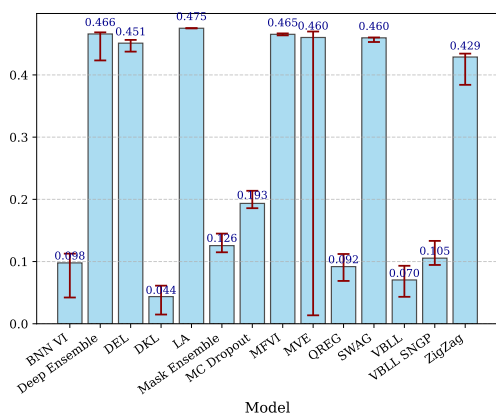


(a) PolyNC

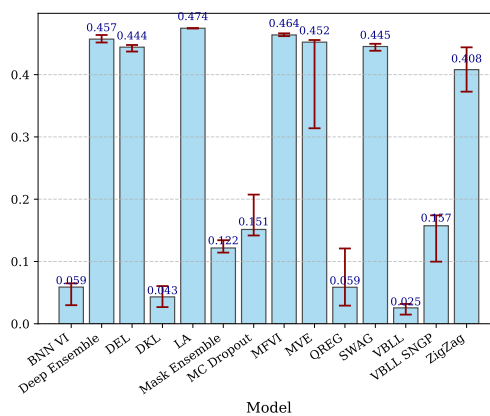


(b) PolyBERT

Figure 9: CRPS values for FFV property of polymers.



(a) PolyNC



(b) PolyBERT

Figure 10: CA values for FFV property of polymers.